Regularization extraction for real-time plasma tomography at JET

D. R. Ferreira[1], D. D. Carvalho[1], P. J. Carvalho[1], H. Fernandes[1], and JET Contributors*

EUROfusion Consortium, JET, Culham Science Centre, Abingdon, OX14 3DB, UK

[1]*Instituto de Plasmas e Fusão Nuclear, Instituto Superior Técnico, Universidade de Lisboa, 1049-001 Lisboa, Portugal*

Introduction

The Joint European Torus (JET) has a vast assortment of diagnostics [2]. In particular, a set of bolometers [3] measure the plasma radiation along multiple lines of sight on a poloidal cross-section of the device. From the measurements of such detectors, it is possible to reconstruct the 2D plasma radiation profile using tomography techniques [4]. The principle is the same as computed tomography (CT) in medical applications, but the techniques are fundamentally different due to the scarce number of lines of sight available.

In fact, plasma tomography is a severely under-determined problem. For example, in JET a tomographic reconstruction may have a resolution of 115×196 pixels, while there are only 56 lines of sight available. A solution to such under-determined problem must involve some form of regularization [5]. One possibility is to enforce smoothness along the magnetic flux surfaces [6]. Another approach is to use prior knowledge from other diagnostics [7]. In addition, an iterative procedure is needed to find the optimal regularization parameters [8]. As a result, tomographic reconstructions have extensive knowledge embedded into them, they are expensive to compute, and such computation can hardly be done in real-time.

In this work, we describe an approach to extract the regularization from existing reconstructions. Based on a set of 800 reconstructions that have been carefully curated at JET, we use a machine learning framework to extract a regularization matrix that shows how, in general, each line of sight contributes to the pixels in a reconstruction. In some cases, the regularization pattern seems to follow the magnetic flux surfaces. More importantly, once the regularization patterns have been found, new reconstructions can be computed in a single matrix multiplication step, thus enabling the use of plasma tomography as a real-time diagnostic.

Fitting the Inverse Matrix

Let $\mathbf{f}$ be a 56-dimensional vector of bolometer measurements, and let $\mathbf{g}$ represent a 115×196 reconstruction of the plasma radiation profile, which is also reshaped into a column vector. We

*See the author list of [1].

call $\mathbf{f}=\mathbf{T}\cdot\mathbf{g}$ the *forward problem*, where $\mathbf{T}$ is a 56×22540 transformation matrix that describes how each pixel in the reconstruction contributes to each detector measurement. Conversely, we call $\mathbf{g}=\mathbf{M}\cdot\mathbf{f}$ the *inverse problem*, where $\mathbf{M}$ is a 22540×56 matrix that describes how each detector measurement contributes to each pixel in the reconstruction.

In general, $\mathbf{T}$ is known from the detector geometry (i.e. from the detector positions and their lines of sight) but it cannot be inverted directly. However, if we have a set of reconstructions $\{\mathbf{g}_1,\mathbf{g}_2,...,\mathbf{g}_n\}$ together with their corresponding measurements $\{\mathbf{f}_1,\mathbf{f}_2,...,\mathbf{f}_n\}$, it is possible to find $\mathbf{M}$ by minimizing the mean absolute error: $L=\frac{1}{n}\sum_i\|\mathbf{g}_i-\mathbf{M}\cdot\mathbf{f}_i\|$.

Since $\mathbf{M}$ represents a large number of parameters, we use a machine learning framework (Theano [9]) to fit $\mathbf{M}$ by gradient descent on a graphics processing unit (GPU). Basically, the update rule at each iteration is given by $\mathbf{M}\leftarrow\mathbf{M}-\eta\cdot\nabla L$ where η is the learning rate and ∇L is the gradient of L with respect to $\mathbf{M}$. In addition, convergence can be accelerated by the use of momentum [10]. With a learning rate of $\eta=0.01$ and momentum $\gamma=0.999$, the loss L converges to a minimum of 0.006 MW/m^3 in 10^6 iterations (53 minutes) on an Nvidia Titan X GPU.

Regularization Patterns

Each value M_{ij} in $\mathbf{M}$ indicates how much detector j contributes to the value of pixel i. Therefore, each column j indicates the contribution of detector j to the whole reconstruction. It is then possible to observe the regularization pattern that $\mathbf{M}$ is enforcing by plotting each column reshaped into the original image size (115×196). Some examples are presented in Figure 1.

The measurements along most lines of sight contribute to curvatures that resemble the magnetic flux surfaces. For other lines of sight pointing directly at the divertor or at the plasma core, the detector contribution is mainly focused on these regions. While the overall shape of the regularization patterns seems plausible, there are some regions with associated regularization that appear to have no relation to their correspondent line of sight. Nevertheless, since the contributions in those regions are relatively small when compared to other detectors, they should not affect the overall quality of the reconstructions.

Quality of the Reconstructions

To evaluate the quality of the reconstructions obtained with $\mathbf{M}$, we divided the dataset into 90% for training and 10% for validation. The validation loss was 0.007 MW/m^3 after 10^6 iterations and showed no sign of overfitting, consistently decreasing with the training loss. To compare the reconstructions produced by $\mathbf{M}$ with the true reconstructions in the validation set, we used image quality metrics such as structural similarity (SSIM), peak signal-to-noise ratio (PSNR) and normalized root mean square error (NRMSE). The average results on the vali-

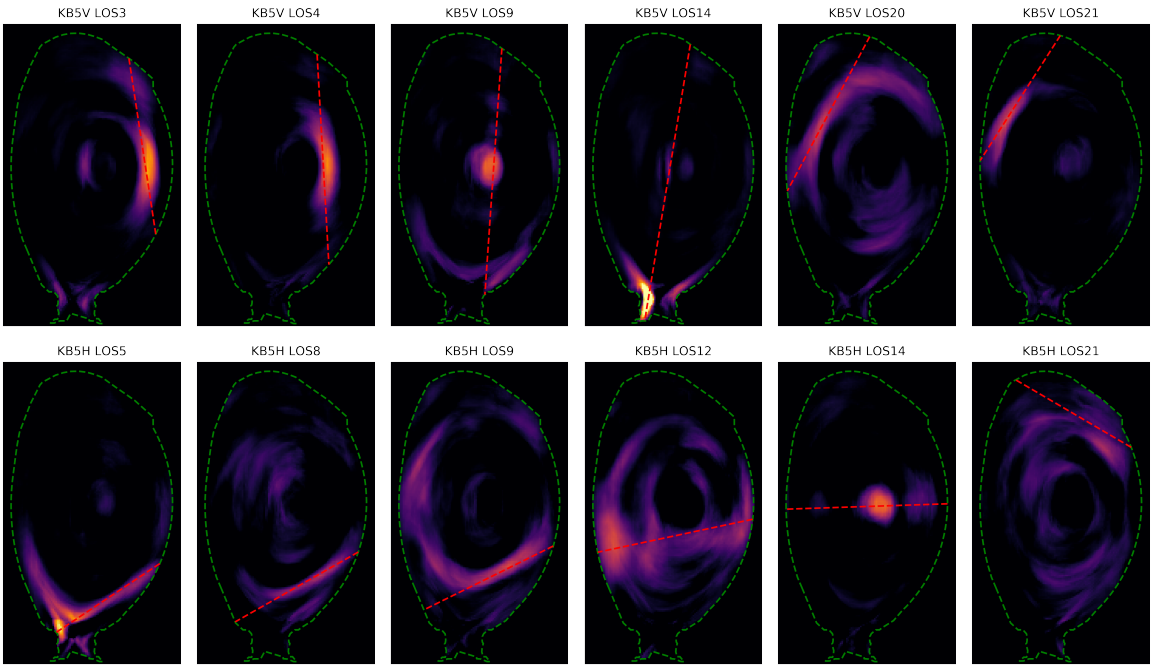

Figure 1: Regularization patterns obtained for different lines of sight (dashed red) of the bolometer system at JET. Vessel contour shown in dashed green.

dation set were SSIM$=0.948$, PSNR$=38.2$ dB, and NRMSE $=0.0435$, with NRMSE being normalized by the intensity range of the true image.

Full-Pulse Reconstruction

Once $\mathbf{M}$ is found, it is possible to compute new reconstructions by simply multiplying $\mathbf{M}$ by the given detector measurements $\mathbf{f}$. For example, doing this with NumPy on a standard quad-core CPU takes 0.4 ms. This is a significant speedup, considering that the original algorithm being used at JET [11] can take several minutes to compute a single reconstruction. With 0.4 ms per reconstruction, it is possible to compute reconstructions in real-time at half the sampling rate of the JET bolometer system (5 kHz). Figure 2 illustrates a full-pulse reconstruction using matrix $\mathbf{M}$. Not only is the method fast, but it also provides similar results to those obtained with more complex models [12].

Acknowledgments

This work has been carried out within the framework of the EUROfusion Consortium and has received funding from the Euratom research and training programme 2014-2018 under grant agreement No 633053. The views and opinions expressed herein do not necessarily reflect those of the European Commission. IPFN activities received financial support from Fundação para a Ciência e a Tecnologia (FCT) through project UID/FIS/50010/2013. The Titan X GPU used in this work was donated by NVIDIA Corporation.

References

[1] X. Litaudon et al., Nucl. Fusion **57**, 10, 102001 (2017)

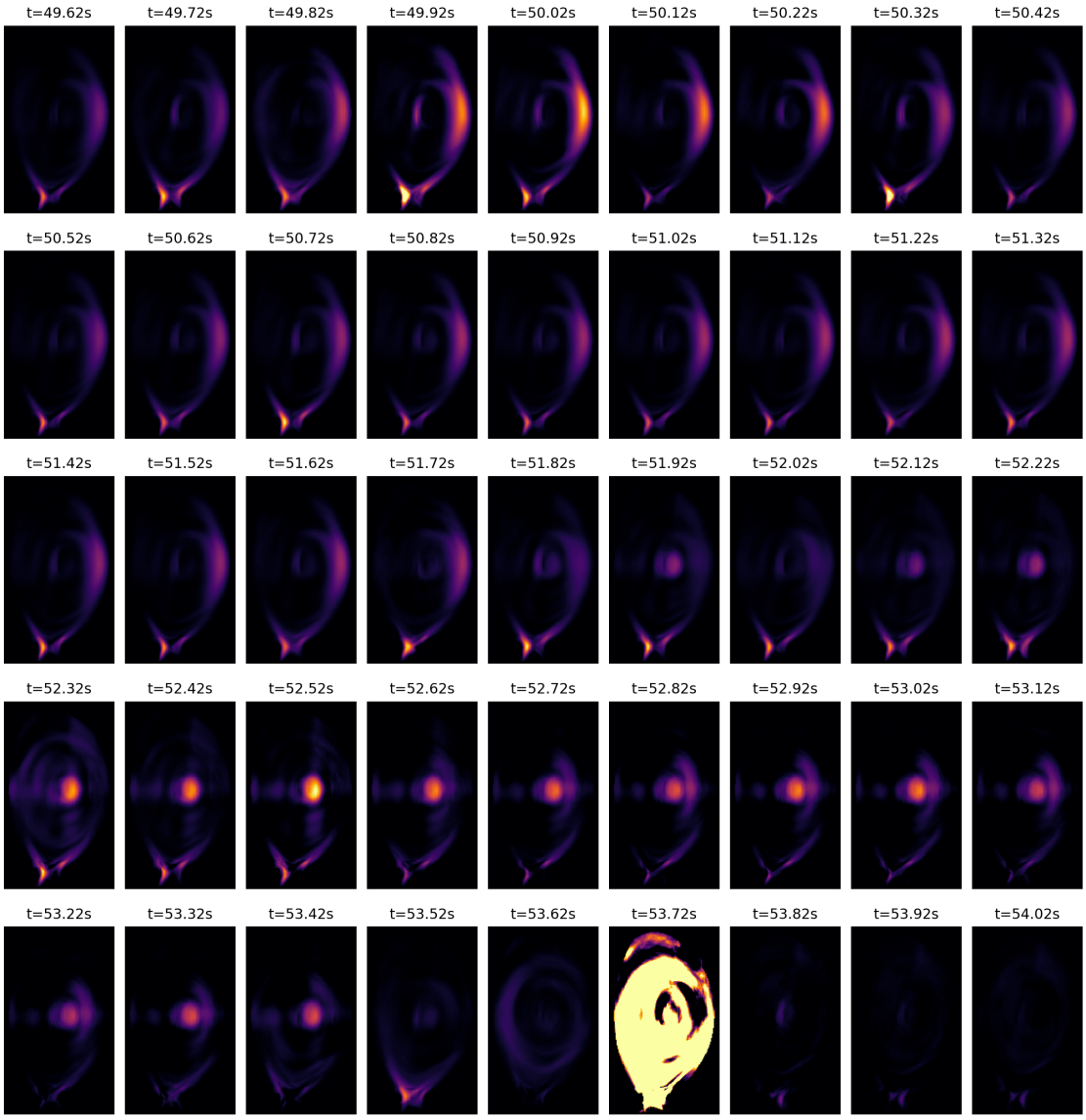

Figure 2: Full pulse reconstruction of shot #92213 from $t = 49.62$ s to $t = 54.02$ s with a time step of 0.01 s (disruption at $t = 53.72$ s)

[2] R. Felton et al., Fusion Eng. Des. **74**, 1, 561 (2005)

[3] A. Huber et al., Fusion Eng. Des. **82**, 5, 1327 (2007)

[4] L. C. Ingesson et al., Fusion Sci. Technol. **53**, 2, 528 (2008)

[5] J. Mlynar et al., Fusion Sci. Technol. **58**, 3, 733 (2010)

[6] M. Odstrcil et al., Nucl. Instrum. Meth. A **686**, 156 (2012)

[7] J. Bielecki et al., Rev. Sci. Instrum. **86**, 9, 093505 (2015)

[8] V. Loffelmann et al., Fusion Sci. Technol. **69**, 2, 505 (2016)

[9] R. Al-Rfou et al., arXiv:1605.02688 (2016)

[10] I. Sutskever et al., ICML'13 (2013)

[11] L. Ingesson et al., Nucl. Fusion **38**, 11, 1675 (1998)

[12] D. R. Ferreira et al., arXiv:1802.02242 (2018)